Pb speciation versus TCLP release in army firing range soils

D. Dermatas, G. Shen*, M. Chrysochoou, D.G. Grubb, N. Menounou, P. Dutko

W.M. Keck Geoenvironmental Laboratory, Center for Environmental Systems, Stevens Institute of Technology, Hoboken, NJ 07030, USA

Available online 18 January 2006

Abstract

A series of soil parameter and mineralogical investigative techniques were applied to assess the Pb speciation in four US Army firing range soils that presented significantly different Pb leaching regimes and soil characteristics. Soil gradation tests were complemented by total chemical analyses, X-ray powder diffraction (XRPD), Rietveld quantification, optical microscopy and scanning electron microscopy (SEM) analyses. The bulk geotechnical, mineralogical and chemical analyses pointed to two possible Pb retention mechanisms: precipitation as lead carbonate and sorption in the case of fine-grained soils. Lead speciation and mobility was further investigated by the toxicity characteristic leaching procedure (TCLP) and sequential extraction test (SET). As the TCLP Pb concentrations did not necessarily reflect the total Pb analysis of the soils, the Pb leachability ratio (TCLP/total) was found to be controlled by soil mineralogy and its response to changes in system pH. Geochemical modeling, using Visual MINTEQ, was employed to evaluate the mechanisms that controlled the observed TCLP Pb leaching behavior. It was found that lead carbonate precipitation/dissolution reactions controlled Pb TCLP leachability in all soils, while sorptive phenomena did not seem to play a role even in the case of fine-grained soils. More specifically, TCLP Pb leachability was controlled by the pH, the available Pb and the available carbonate in solution. This indicates that geochemical modeling strongly complimented TCLP Pb analyses. Thus, geochemical modeling is an important assessment tool to evaluate the magnitude of site-specific Pb-related environmental problems in firing range soils. Carbonation reactions, involving metallic Pb, that occur during the SET obscure its ability to reliably ascertain Pb speciation. More specifically, SET lumps the extractable Pb into predetermined phase categories that may not be truly representative of the actual soil mineralogy or dominant forms of Pb in the soil. A thorough geotechnical, mineralogical and chemical investigation of firing range soils, complemented by geochemical modeling, was therefore found to be a more reliable approach to evaluate Pb speciation and TCLP release in firing range soils.

1. Introduction

Following impact, Pb bullets may be oxidized and otherwise chemically transformed to soluble species in soil environments. The amount and rate of Pb weathering and its subsequent release into the soil environment depends on both soil properties and the ammunition composition. Pb release was found to be affected by soil pH, soil organic matter and the cation exchange capacity (CEC) of the soil [1]. Dermatas et al. [2] found that soil and Pb metallic fragment particle sizes played a dominant role in the rate and amount of Pb release. They also found that Pb release was affected by soil pH, buffering capacity and mineralogy. The presence of binding surfaces in clays, organic matter and ferromanganese oxides has been reported as responsible for Pb retention in several studies [3–6]. Lin et al. [7] observed that

gibbsite [$Al(OH)_3$] was an effective sink for Pb in firing range soils in Central Sweden owing to specific adsorption and/or co-precipitation reactions. Jorgensen and Willems [8] found that metallic Pb in shotgun pellets fired at Danish shotgun ranges was rapidly transformed to hydrocerussite [$Pb_3(CO_3)_2(OH)_2$], cerussite [$PbCO_3$] and anglesite [$PbSO_4$]. Lin et al. [7] observed the same minerals on weathered Pb fragment surfaces. Cao et al. [9,10] identified cerussite and hydrocerussite deposits on bullet fragments as well as pyromorphite [$Pb_{10}(PO_4)_6(OH)_2$], an insoluble lead phosphate mineral, in high phosphate content firing range soils in Florida (USA). Dermatas et al. [2,11] also identified cerussite, hydrocerussite, anglesite and litharge [PbO] on Pb bullet fragments.

In spite of the extensive research on Pb occurrence, fate and transport in firing range soils, it remains a challenge to explain the rather large range of values of Pb concentrations and release rates reported in the literature. Based on a comprehensive literature review on Pb corrosion in soils, Scheinost [12] reported that typical chemical soil parameters cannot fully

---

* Corresponding author. Tel.: +1 201 216 5432; fax: +1 201 216 8212.
 E-mail address: gshen@stevens.edu (G. Shen).

explain the large variation (i.e., four orders of magnitude) of reported Pb weathering rates in soil environments. Without a comprehensive understanding of the mechanisms responsible for such large variations in reported Pb release values, it may be difficult to adequately address the environmental concerns associated with the use of Pb during firing activities. In an attempt to resolve some of these issues, the present study compares two techniques used to evaluate Pb leaching and mobility in firing range soils: the toxicity characteristic leaching procedure (TCLP) and sequential extraction test (SET) procedures. The TCLP test was used to determine if the shooting range soils are designated as a hazardous waste against the USEPA TCLP leaching criteria (5 mg/L) for lead, i.e., the regulatory driver for site remediation. SET results on firing range soils illustrated that Pb leachability was highest when Pb was primarily associated with the carbonate fraction of the soil [9], versus when Pb occurred in the organic matter [6] or soil residual fractions [9]. This finding would seem to contradict general Pb geochemistry principles—metallic Pb and other "difficult-to-leach" Pb forms should mostly be associated with the soil residual fractions of the SET. Conversely, the presence of organic matter may actually favor higher levels of Pb TCLP leachability, as Pb complexation reactions may accelerate weathering reactions and Pb mobility.

Recognizing the importance of the various soil attributes on Pb weathering and subsequent mobility, four different firing range soils were selected as they represent a wide range of relevant soil properties and parameters, namely soil pH, grain size distribution, mineralogy and composition. The selected soils were tested for: (1) basic soil parameters (water content, soil pH and grain size distribution); (2) mineralogy (qualitative and quantitative X-ray powder diffraction—XRPD); (3) micromorphology (scanning electron microscope—SEM and optical microscopy techniques); (4) chemical composition including total concentration of Pb and major metals (total analyses), and organic matter and carbonate contents; (5) Pb leaching behavior (TCLP and SET). Based on these experiments, the TCLP and SET Pb release regime was obtained and the soil-specific mechanisms responsible for Pb mobility were identified. Geochemical modeling was also performed to confirm the controlling mechanisms of TCLP Pb leachability and assess the overall accuracy of model-based predictions.

2. Materials and methods

2.1. Soil sampling

Soil samples were taken within the zone of bullet penetration from the surface and near surface of berms (backstops) at four different firing ranges: Goldstone Site (Mojave Desert, California—FIGS) and three New Jersey (NJ) army training facilities: the Armaments Technology Facility (PATF), the Marine Range (PAMR) (both are indoor facilities located at Picatinny Arsenal, Dover, NJ) and the outdoor Fort Dix Range 15 (FDR15) site located in South New Jersey. Overall, both geographical location and soil characteristics (e.g. type of parent soil, soil pH, presence of salts, grain size and mineralogy)

varied greatly among these firing range soils. All sites are active ranges except the Goldstone (FIGS), which was abandoned in 1972. With the exception of the FIGS soil (i.e., residing in a desert, evaporitic environment), the other firing range soils did not contain significant amounts of salt precipitates. All soil samples were first homogenized through a sample splitter to obtain representative material. Unless otherwise noted, the collected soil samples were then air-dried at the room temperature and passed through No. 4 sieve (4.75 mm) prior to all testing.

2.2. Geotechnical parameter analyses

Soil moisture content, soil pH and particle size distribution were measured in accordance with ASTM D2216-92, ASTM D4972-89 and ASTM C136-96A, respectively [13]. Soil classification was determined using the Unified Soil Classification System (USCS).

2.3. Mineralogical soil analyses

Soil mineralogy and Pb weathering products were investigated using optical microscopy with a Nikon optical microscope (SMZ-1000) and XRPD analysis with a Rigaku DXR 3000 computer-automated diffractometer. SEM analyses were also performed to examine the morphology of the metallic Pb transformation products and to conduct microanalyses of soil samples.

2.3.1. X-ray powder diffraction(XRPD)

Samples were air-dried for 24 h, passed through a U.S. Standard No. 4 sieve (4.75 mm), and mechanically pulverized to pass a U.S. Standard No. 400 sieve (38 μm). Step-scanned XRPD data were collected using Bragg–Brentano geometry. The diffractometry was conducted at 40 kV and 30 mA using a diffracted beam graphite-monochromator with Cu radiation. Unless otherwise noted, data were collected in the range of two-theta values between 5° and 65° with a step size of 0.05° and a count time of 5 s per step. XRPD patterns were analyzed by the Jade software, Version 7.1 [14] and referenced to the patterns of the International Centre for Diffraction Data Database [15], as well as the Inorganic Crystal Structure Database [16]. Quantitative phase analysis by the Rietveld method [17] was conducted using the Whole Pattern Fitting function of Jade. The detection limit of XRPD and the accuracy of the quantitative analysis of XRPD patterns by the Rietveld method depend on instrumental parameters, the degree of crystallinity of the mineral phases and the overall pattern complexity. A rough estimate for the XRPD detection limit is 3–5%, but cases have been reported, in which phases were detected down to 0.1%. With respect to the accuracy of Rietveld, especially in the presence of amorphous material and for phases below the XRPD detection limit, errors can be significant. However, Rietveld provides a reliable tool for estimating the relative distribution of the quantified mineral phases. More specifically, in the absence of significant amorphous material presence, the absolute errors for the quantified phases are estimated at 5–10% for the major phases (i.e., quantity >20%) and 3% for minor phases.

Table 1
Summary of the "Tessier" SET method

Hypothesized soil fraction attacked	Chemical used	Duration (h)
Loosely sorbed (e.g., on clays)	1 M $MgCl_2$, pH 7, 25 °C, 8 mL/1 g soil	1
Carbonates some hydroxides	1 M CH_3COONa, pH 5, 25 °C, 8 mL/1 g of soil	5
Mn and Fe oxides	0.04 M $NH_2OH·HCl$, in 25% (v/v) CH_3COOH, 96 °C, 20 mL/1 g of soil	6
Organics and sulfides	30% H_2O_2, pH 2 with HNO_3, 1.2 M CH_3COONH_4, 85 °C, 20 mL/1 g of soil	5
Residual	EPA Method 3050B[a]	–

[a] EPA Method 3050B was adopted for the residual step of the "Tessier" extraction method for safety purposes (vs. HF acid), which provides a comparable result in our experience.

2.3.2. Scanning electron microscopy/energy dispersive X-ray (SEM/EDX)

Air-dried samples were mounted using double-sided carbon tape and non-conductive samples were gold coated. All samples were analyzed by SEM/EDX using a LEO 982 field emission SEM with an Oxford energy dispersive X-ray analyzer.

2.4. Total organic carbon analyses

Soil samples were sent to Galbraith Laboratories Inc. in Knoxville, TN, for total carbon, carbonate and total organic carbon analysis using the Wet Oxidation Method [18].

2.5. Chemical soil analyses

All chemical soil analyses were performed by a Varian Vista-MPX inductively coupled plasma-optical emission spectroscopy (ICP-OES), unless otherwise noted. A number of blanks, replicates, spikes and a certified reference material (NIST 2170) were tested with each batch of samples for quality control purposes. Total metal concentrations were measured according to USEPA Method 3050B [19] which entailed the following steps: (i) concentrated nitric acid was used to digest 1 g of the dry sample at 96.5 °C; (ii) varying amounts of H_2O_2 (up to 10 ml) were added to the sample to extract metals from the soil organic matter fraction; (iii) the solution was diluted to 100 mL and filtered for analysis. Pb leachability was evaluated using the TCLP–EPA Method 1311 [20]. Two acetic acid based TCLP extraction fluids were prepared: extraction fluid No. 1 (pH 4.93 ± 0.05) and extraction fluid No. 2 (pH 2.88 ± 0.05). Fluid No. 1 was used when the pH of the slurried sample was less than 5. Fluid No. 2 was applied when the slurry pH was above 5 and remained so after the addition of 1N HCl. However, when the pH dropped below 5 upon HCl addition, fluid No. 1 was used. Therefore, both soil pH and buffering capacity were considered when making the extraction fluid selection. After 18 h of mixing in a TCLP tumbler, the leachate was filtered using a Millipore 0.4 μm filter. The pH of the filtrate was then measured and the leachate was acidified with a small amount of nitric acid to a pH less than 2, followed by ICP-OES analysis.

Pb partitioning in different soil fractions was also evaluated using the Tessier SET method [21]. Tessier's SET method involves exposing soils to a series of successively more aggressive chemical fluids to release metals from sediments and sediment-like media. The leaching is performed sequentially on sample residuals from the previous step. Each extraction is believed to affect primarily one or more physical phases of the soil, which are "operationally" defined as the: (a) exchangeable (EX), (b) carbonate (CB), (c) Fe–Mn oxides (FM), (d) organic matter and sulfides (OS) and (e) residual soil (RS) phases. Table 1 presents the reagents and conditions used for each step as well as a description of the different fractions involved.

2.6. Modeling

The Visual MINTEQ software [22] was used to compare the theoretical Pb leaching (versus the actual) from each firing range soil in a closed aqueous system based on its: (i) initial ion concentrations (mg/kg solid), such as for Pb, Al, Ca, Fe and Mn (Table 4); (ii) total carbonate content (Table 4); (iii) a liquid to solid (L:S) ratio of 20 in order to simulate the TCLP dilution factor; (iv) final TCLP pH value measured in the filtrate after tumbling the slurry for 18 h; (v) a sulfate concentration of 19,000 mg/kg for the FIGS soil, because gypsum ($CaSO_4·2H_2O$) was identified in the bulk XRPD pattern. The gypsum quantity was estimated by Rietveld, but was halved owing to the FIGS amorphous content. Oversaturated solids were allowed to precipitate and varying the initial sulfate concentration did not affect the modeling results.

3. Results and discussion

It is important at the outset of this section to indicate that no single tool or approach currently used in the evaluation of metals leaching from firing range soils can accurately account for leaching phenomena due to the many processes involved. The strategy adopted here is to use multiple lines of evidence to develop an understanding of actual phenomena, and to nevertheless develop that understanding given the limitations of the individual investigation techniques. Accordingly, the results and discussion are combined, integrated and contextualized because one tool may yield misleading results when considered alone.

3.1. Geotechnical parameters of the firing range soils

The water content, pH and particle size distribution of the soils tested are presented in Table 2. Three out of the four soils were characterized as neutral to alkaline pH (7.5–8.7), whereas the Range 15 soil (FDR15) was acidic (pH 4.4). In soil environments, low pH generally corresponds to a high potential for Pb release, however, soil buffering capacity must also be considered especially when regulatory (i.e., TCLP) Pb release is

Table 2
Selected geotechnical properties of the range soils

Firing ranges	Water content (%)	Soil pH (1:1) water to soil	Gravel[a] (%)	Sand[a] (%)	Fines[a] (%)	USCS symbol
FIGS	5.8	7.5	5.2	6.1	88.7	CL-ML
PATF	4.0	8.7	6.7	74.3	19.0	SM
FDR15	4.2	4.4	1.9	90.8	7.3	SW-SM
PAMR	0.1	8.7	7.3	87.9	4.8	SW

S: sand; C: clay; M: silt; L: low plasticity; W: well graded.

[a] Sieve opening for gravel: 75–4.75 mm, sand: 4.75 mm to 75 μm, fines: <75 μm.

concerned. The water contents of the selected soils were generally low (<6%), so water content was not considered as a variable for the purposes of the present study. Generally, lower water contents would favor lower rates of Pb weathering and subsequent release.

The FIGS soil was classified as a silty clay or lean clay soil (∼89% fines) by the Unified Soil Classification System. The FIGS soil pH reflects its desert, evaporitic depositional environment. The high amount of fines in the FIGS soil would indicate a relatively high potential for this soil to bind Pb by sorption and other surface processes. The PATF indoor range soil was categorized as a silty sand, the 19% fines indicating a significant potential for Pb immobilization. The PATF soil mainly contained dredge sands, which were very susceptible to pulverization upon repeated bullet impact and have thus contributed to its elevated fines content. Specifically, sea shells, micas, as well as decomposed granite were observed within the PATF soil. The FDR15 soil was classified as a well graded high quartz sand with some silt, with 7.3% fines, indicating a limited potential for Pb immobilization. The PAMR indoor range soil was categorized as a well graded sand with minimal fines (4.8%), again indicating a very low potential to bind Pb unless its mineralogy revealed otherwise. More important than the fines content of these soils is their mineralogy, which has the ability to dominate Pb retention and leaching. Accordingly, detailed mineralogical investigations were completed for each soil, as described in the following section.

3.2. Mineralogical characteristics of the firing range soils

The mineralogy of the firing range soils was examined using XRPD and the identified phases were quantified using the Rietveld method with Jade. Selected samples were also analyzed by optical and electron microscopy. Table 3 presents the results of mineral quantification.

The bulk mineralogy of the FIGS soil included quartz, feldspars and mica (muscovite), with smaller amounts of gypsum, calcite and cristobalite. The major clay identified was kaolinite (5.8%), along with minor amounts of montmorillonite (3.2%). Of the mineral phases quantified, only montmorillonite (and to a lesser degree kaolinite) would have significant potential to bind Pb through sorption and cation exchange. The presence of poorly crystallized and/or amorphous mineral phases was also observed by XRPD (Fig. 1) but could not be reliably quantified by Rietveld. The amorphous humps at a two-theta value of 26.7° may indicate the presence of amorphous silica, while the amorphous peak around the peak at 35° suggests the presence of amorphous iron oxides and/or hydroxides (most likely FeOOH). In order to include the presence of amorphous iron oxides in the quantification, the phases hematite and magnetite were included in the Rietveld refinement. It should be stressed, however, that the estimated quantity for these phases should be evaluated as indicative, as the significant peak overlap in the two-theta interval 34–38° renders the quantification of the aforementioned phases difficult. Overall, the significant pattern

Table 3
Major soil minerals detected in the selected firing range soils by XRPD

Major minerals	Chemical formula	JCPDS no.[a]	FIGS	PATF	FDR15	PAMR
Quartz	SiO_2	46–1045	13.8	79.9	100	10.2
Cristobalite	SiO_2	39–1425	3.0			
Feldspar	$(Ca,Na)(Si,Al)_4O_8$	41–1480	37.2	6.9		16.6
Muscovite	$(K,Na)(Al,Mg,Fe)_2(Si_3Al)O_{10}(OH)_2$	07–0025	23.2	6.5		9.5
Sodium mica	$NaAl_3Si_3O_{11}$	46–0740		5.4		7.0
Calcite	$CaCO_3$	05–0586	4.8	0.9		41.4
Dolomite	$(Ca,Mg)CO_3$	36–0426				12.2
Kaolinite	$Al_2Si_2O_5(OH)_4$	29–1488	5.8			
Montmorillonite	$Ca_{0.2}(Al,Mg)_2Si_4O_{10}(OH)_2\cdot4(H_2O)$	13–0135	3.2			
Lead	Pb	04–686				2.2
Cerussite	$PbCO_3$	47–1734		0.4		
Gypsum	$CaSO_4$	33–0311	6.8			
Hematite	Fe_2O_3	33–0664	0.6			
Magnetite	$Fe^{2+}Fe_2^{3+}O_4$	19–0629	1.0			
Cordierite	$Mg_2Al_4Si_5O_{18}$	13–0294	0.7			0.9

All values are on a dry weight basis (%).

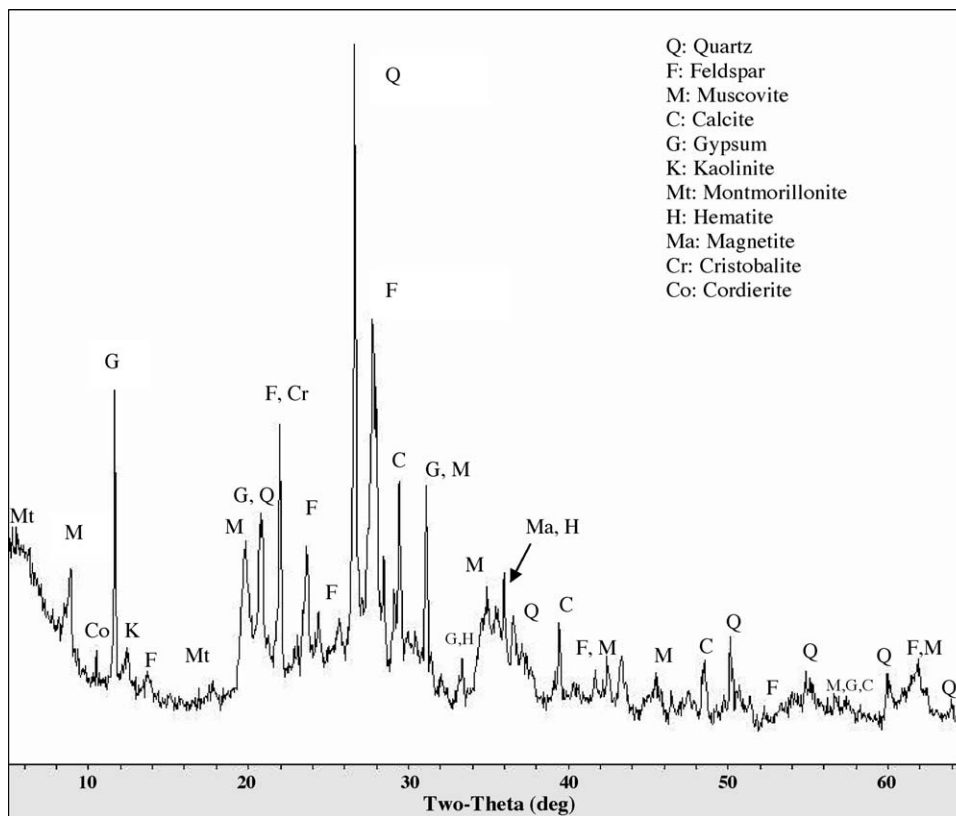[a] Refers to XRPD data files used by ICDD.

Fig. 1. XRPD pattern of the FIGS firing range soil.

complexity and presence of amorphous material of the FIGS soil increases the uncertainty in Rietveld quantification. However, the relative distribution of the identified minerals may be employed as an accurate depiction of the prevailing soil mineralogy. Pb compounds were not observed in the FIGS soil, probably due to the low total Pb level that would render its crystalline compounds non-detectable by XRPD. Alternatively, Pb could be sorbed on the clay and/or ferromanganese oxide surfaces; again, it would not be detected by XRPD in its sorbed form. However, in previous studies, an examination of Pb corroded fragments collected from the FIGS soil indicated that the main Pb transformation products were lead carbonates (i.e., cerussite and hydrocerussite), even though some anglesite [$PbSO_4$] and litharge [PbO] were also identified [2,11].

The XRPD analysis of the PATF soil yielded a pattern with good resolution and no significant amorphous humps. It mainly consisted of quartz ($\sim$80 wt%), which agrees with the high sand content (Table 2). About 0.4% of cerussite [$PbCO_3$] was identified in the PATF soil (Table 3), along with some micas and feldspars and a small amount of calcite. Based on the bulk XRPD results, there were no mineral phases with potential Pb binding surfaces quantified in the PATF soil. A closer examination of the PATF soil under the optical microscope revealed the presence of bayerite [$Al(OH)_3$] and boehmite [$AlOOH$] (referred sometimes also as pseudoboehmite), polymorphs of aluminum hydroxide (like gibbsite but colored blue; Fig. 2a). This finding was also confirmed by XRPD analysis of selected blue particles (Fig. 2b). Aluminum hydroxides, similar to gibbsite, have a high

potential for Pb sorption [7]. Fig. 2b shows that boehmite existed in a poorly crystallized and/or amorphous state (i.e., boehmite peaks are broad and noisy), thus indicating the higher potential, as compared to bayerite, for this mineral phase to bind Pb. Further analysis by SEM also confirmed the presence of cerussite (lead carbonate) on the surface of weathered metallic Pb particles (Fig. 2c). It should be noted, however, that the presence of cerussite in the bulk soil, as it was identified by XRPD, would suggest that lead carbonate was possibly also present as a through-solution precipitate. Similar to aluminum hydroxides, ferromanganese oxides can also provide available sorption sites for Pb. Moreover, the presence of cerussite and aluminum hydroxide reflects the relatively high PATF soil pH (Table 2).

The FDR15 soil contained only quartz which is not expected to significantly contribute to Pb binding by surface processes. Similar to FIGS and PATF, when Pb corroded fragments were closely examined and then analyzed by XRPD, cerussite was the only Pb transformation product identified, as shown in Fig. 3.

XRPD results from the PAMR soil showed significant quantities of calcite and dolomite (>50%), along with some lower amounts of feldspars and micas, as well as traces of cordierite (Table 3). Pb was identified in its metallic form, and the presence of calcite and dolomite was confirmed by means of optical microscope observations (Fig. 4). The high calcite and dolomite content suggested a potentially high soil buffering capacity and thus was also reflected by the relatively high PAMR soil pH (Table 2). Some Pb sorption onto calcite and dolomite mineral surfaces is also possible, albeit the coarse-grained nature of the
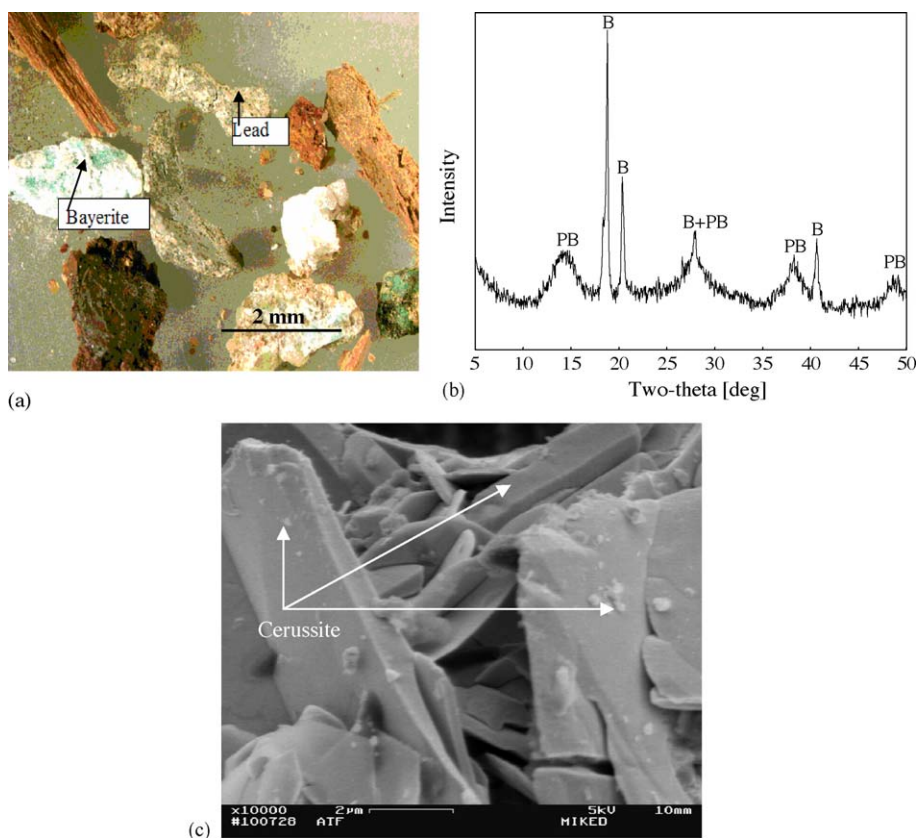
Fig. 2. (a) PATF sample optical microscope image showing particles of bayerite–boehmite (blue) and weathered Pb bullet fragments (with white surface coating of cerussite). (b) XRPD pattern of blue particles from PATF soils confirming bayerite and boehmite. PB—pseudoboehmite (another name for boehmite) and B—bayerite. (c) SEM image close-up of PATF soil sample showing cerussite crystal formation on Pb bullet fragment surfaces. (For interpretation of the references to color in this figure legend, the reader is referred to the web version of the article.)

PAMR soil. The significant presence (2.2%) of metallic Pb and the fact that no cerussite (lead carbonate) was visually detected in the bulk sample (i.e., during the screening process) indicated a lower rate of Pb weathering for this soil. It should be noted, however, that in a previous study, metallic Pb fragments were found to be covered by cerussite surface coatings, similar to FIGS, PATF and FDR15 [11].

Overall, the Rietveld analysis accurately reflects and compliments the results of the soil gradation analyses, i.e., the high fines fraction in the FIGS soil is reflected in the high feldspar and clay content, while the PATF and FDR15 soils exhibit high amounts of quartz and the PAMR soil calcite and dolomite, which constitute the coarse fraction of these soils. These observations validate the qualitative and quantitative analysis of the obtained XRPD patterns. Furthermore, targeted optical and electron microscope analyses complemented XRPD results by pointing to the presence of poorly crystalline phases and revealing particle associations that can impact Pb speciation and the degree of Pb
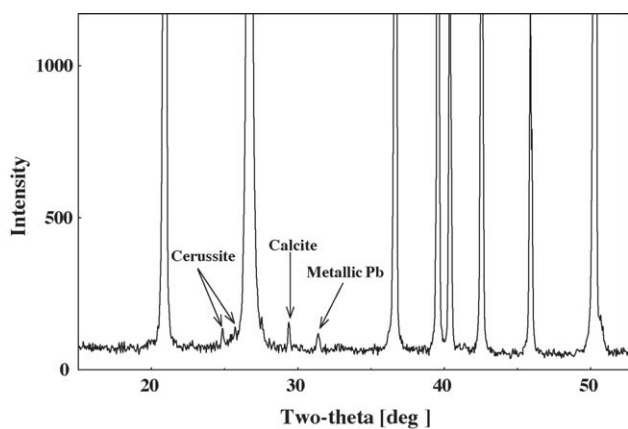

Fig. 3. XRPD pattern of weathered bullet crust material from the FDR15 soil (major minerals presented were quartz (large peaks) with smaller amount of calcite, cerussite and metallic Pb).
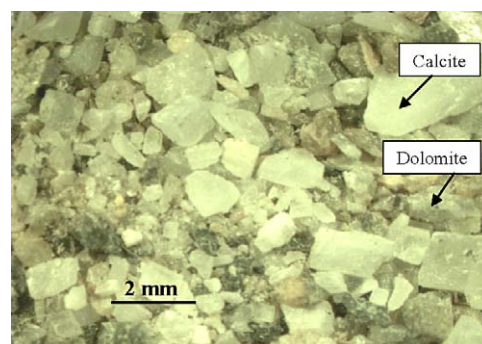

Fig. 4. Optical microscope image of a PAMR soil sample, showing ubiquitous calcite and dolomite crystals.

Table 4
Major elements, Pb concentrations, carbonate and organic content in firing range soils

Firing ranges	Al	Ca	Fe	Mg	Mn	Pb	Carbonate	Organic carbon
FIGS	43151	33186	30980	20105	660	3165	4800	4300
PATF	10644	3511	15638	1385	148	27417	3600	5000
FDR15	2407	203	1978	60	6	1025	100	1600
PAMR	2247	235044	5562	17010	252	49228	378000	7000

All data in mg/kg.

weathering. Specifically, for all the firing range soils, the controlling metallic Pb transformation mechanism was identified as carbonation, resulting in the formation of lead carbonate (cerussite). Cerussite may form both topochemically, in the form of surface coatings on metallic Pb fragments as evidenced in all firing range soils (Fig. 2a), and as precipitates from solution as evidenced in the PATF soil (Fig. 2c). For the soils containing significant amounts of fines (FIGS and PATF), the presence of clay, ferromanganese oxides and aluminum hydroxides provide additional reactive surfaces that could sorb Pb.

3.3. Chemical analyses on firing range soils

3.3.1. Total analyses

Total metal concentrations in the firing range soils for iron (Fe), aluminum (Al), calcium (Ca), magnesium (Mg), manganese (Mn) and lead (Pb) are summarized in Table 4. The sixth column in Table 4 demonstrates that all firing range soils exceeded the regulatory Pb screening levels set by the states of California (1000 mg/kg) and New Jersey (400 mg/kg). The two indoor ranges (PATF and PAMR) had the highest Pb concentrations, with 2.74 wt% and 4.92 wt%, respectively. This finding highlights the fact that indoor ranges may have a higher potential to concentrate Pb, which seems counter intuitive until the dust suppression (water spraying) systems in use are considered. In open ranges, Pb can be dispersed from the berm or backstop area as airborne particulates, dissolved or suspended soils in surface water and groundwater flows. The frequency of firing range use and maintenance would also play important roles in Pb accumulation.

Chemical analyses of the FIGS soil revealed relatively higher Al, Fe and Mn contents (43,151 mg/kg, 30,980 mg/kg and 660 mg/kg, respectively) compared to the other firing range soils. The Mg content was also relatively high (20,105 mg/kg) in the FIGS soil, suggesting the presence of $MgCl_2$, though it was not clearly identified by XRPD (no well-defined peaks at 15° or near 35°). Similarly, the presence of amorphous goethite [FeOOH] and some manganese oxide [Mn_2O_3] were also hypothesized based on the total analyses results and mineralogical information obtained. Al-bearing phases, such as clays, as well as amorphous and/or poorly crystallized iron and to a lesser extent manganese oxides (whose presence was indicated by the amorphous humps in the XRPD pattern), would constitute available binding surfaces in the FIGS soil. The Al, Fe and Mn concentrations were also relatively high in the PATF soil (10,644 mg/kg, 15,638 mg/kg and 148 mg/kg, respectively); pointing to the possible presence of Fe and Mn oxides or hydroxides, feldspars and

aluminum hydroxides (i.e., bayerite and boehmite) as shown Fig. 2a and b.

Since the FDR15 soil was composed of pure quartz sand (Table 3), Ca, Fe, Mg and Mn concentrations were not elevated, suggesting a low affinity for Pb immobilization. The Ca and Mg contents of the PAMR soil (Table 4) reflect the presence of calcite and dolomite (Table 3), high soil buffering capacity, and a variety of surfaces for Pb adsorption and/or co-precipitation.

In summary, total analyses support the quantitative mineralogical data for all firing range soils. They also suggest that ferromanganese oxides/hydroxides and $MgCl_2$ may be the amorphous phases underneath the "humps" in the FIGS XRPD pattern (Fig. 1) and point to the presence of aluminum hydroxides and ferromanganese oxides/hydroxides in the PATF soils, all of which may play an important role in controlling Pb leachability.

3.3.2. Organic matter and carbonate content

In order to evaluate the effects of soil organic matter on Pb leachability, the organic carbon content of the firing range samples was determined (Table 4). The carbonate content was relatively low in the FIGS and PATF soils and very low in the FDR15 soil. The carbonate content in the FIGS soil was likely associated with the presence of calcite, while the carbonate content of the PATF soil reflects the presence of both calcite and cerussite (Table 3). The high carbonate concentration in the PAMR soil is consistent with the presence of abundant calcite and dolomite in this soil (Table 3). The organic carbon contents for all the firing range soils were quite low, and should not have major implications for Pb leachability.

3.3.3. TCLP leaching data

The TCLP Pb concentrations for all the firing range soils exceeded the USEPA hazardous waste criteria of 5 mg/L, ranging from 10 mg/L to 594 mg/L. However, the highest TCLP Pb concentrations were not observed in the soils with the highest total Pb concentrations (i.e., the PAMR soil). In order to comparatively evaluate the firing range soil TCLP leachability, the Pb leachability ratio was calculated by dividing the TCLP Pb value by the total Pb concentration. TCLP Pb concentration values were normalized to mg/kg by multiplying the TCLP values by 20, i.e., the L:S ratio of the TCLP extraction. This leachability ratio accurately depicts the composite "extractability" of Pb from the soil matrix as it reflects all contributions to Pb immobilization, not just one mechanism. As such, a high TCLP leachability corresponds to weak immobilization. The highest Pb leachability ratio (97.9%) was observed in the FDR15 soil (Table 5), followed by the PATF soil (43.3%), the FIGS soil

Table 5
TCLP Pb, total Pb and TCLP/total Pb leachability ratios in firing range soils

Firing ranges	Selected TCLP E.F.[a] pH	Original soil pH[b] (1:1) water to soil	P.T.[c] (leaching) pH	TCLP Pb (mg/kg)	Total Pb (mg/kg)	Leachability ratio (%) (TCLP to total Pb)
FIGS	4.93 ± 0.05	7.5	5.8	16.5	3165	10.4
PATF	4.93 ± 0.05	8.7	5.4	594	27417	43.3
FDR15	4.93 ± 0.05	4.4	4.9	50.2	1025	97.9
PAMR	2.88 ± 0.05	8.7	6.2	10.7	49228	0.4

[a] E.F.: extraction fluid.
[b] S:L = 1:1.
[c] P.T.: post-tumbling.

(10.4%) and the PAMR soil (0.4%). Interestingly, the highest Pb leachability ratio occurred in the sample containing the lowest total Pb concentration (FDR15; Table 4), while the lowest Pb leachability ratio was observed in the sample with the highest amount of total Pb (PAMR). This suggests that each soil has a different affinity for Pb, in that different Pb immobilization mechanisms may hold sway. Accordingly, to gain insight on Pb leaching behavior geochemical modeling and sequential extraction testing were undertaken, as discussed below.

3.3.4. Modeling

Table 6 presents the actual TCLP Pb results versus the Visual MINTEQ predicted TCLP leaching as a function of TCLP post-tumbling pH, predicted precipitate and Pb leachability ratio. Overall, the model-predicted values were in general within one order of magnitude of the actual Pb TCLP leaching values, though the model seems to somewhat under-predict Pb leachability. Nevertheless, the results help to ground truth the overall interpretation of Pb speciation when taking into account the inherent pH shifts, kinetic and sample variability issues, as well as limitations of the model itself. That Visual MINTEQ under-predicts actual leaching limits its capacity as a substitute for actual TCLP testing to establish compliance with USEPA regulatory criteria.

The greatest difference in fit between the actual and model-predicted TCLP values occurs with the PAMR soil. The XRPD of the TCLP residue (Fig. 5) confirmed the presence of cerussite and residual metallic Pb, whereas the model only predicted the occurrence of cerussite. Moreover, as calcite and dolomite serve as the primary carbon source in a closed TCLP system, the aqueous carbonate concentration was both restricted by Henry's Law and the contact time (18 h). This suggests that Pb, calcite and dolomite dissolution were kinetically inhibited and the standard contact time (18 h) of the TCLP may not reflect an equilibrium condition. Further support for this conclusion is derived from a complementary research study that showed the

TCLP Pb concentration in the PAMR soil reached an equilibrium value of 0.3 mg/L over an extended contact time (68 h), thus confirming the model prediction. Other studies have also challenged the suitability of the TCLP for the same reasons [23–26]. Cerussite controlled Pb leachability in the PAMR soil to very low levels (0.01% of the Pb remained in solution according to the model), mainly because the calcite- and dolomite-induced high soil buffering capacity effectively maintained the pH at a relatively high value (6.2). As such, there was ample aqueous carbonate to react with aqueous Pb and/or metallic Pb surfaces to form fresh cerussite. Cerussite forming on metallic Pb surfaces has the potential to kinetically control Pb dissolution [11].

Like the PAMR soil, Dermatas et al. showed that equilibrium was not necessarily achieved in the PATF soil after the first 18 h of tumbling. While the amounts of Pb (Table 4) and calcite (Table 3) were lower than the PAMR soil, Pb seemed to be partly precipitated as cerussite (lead carbonate) prior to TCLP testing, suggesting that equilibrium should have been achieved in a shorter timeframe as compared to PAMR. Consequently, even though some degree of kinetic inhibition may also apply to the PATF soil, it was not as significant as compared to the PAMR soil. However, it was found that the actual TCLP Pb concentration was essentially predicted by the model when small variations in the total Pb concentration, carbonate concentration or pH were considered. Specifically, a brief sensitivity analysis indicated that independently increasing total Pb to 3.0%, decreasing the carbonate concentration to 0.30% or decreasing the pH by 0.1 units were each sufficient to allow the model to achieve results very close to the actual TCLP concentration. Overall, sample variability and experimental uncertainties and to a lesser extent kinetic restraints can adequately explain the difference between the actual and the predicted Pb concentrations for the PATF soil. Based on the model, lead carbonate was also predicted to form in the PATF soil in its hydrated form (hydrocerussite instead of cerussite). The reason for the predominance of hydrocerussite in this case is probably related to the ratio of

Table 6
Comparison between actual TCLP Pb and MINTEQ predicted TCLP Pb concentrations in firing range soils

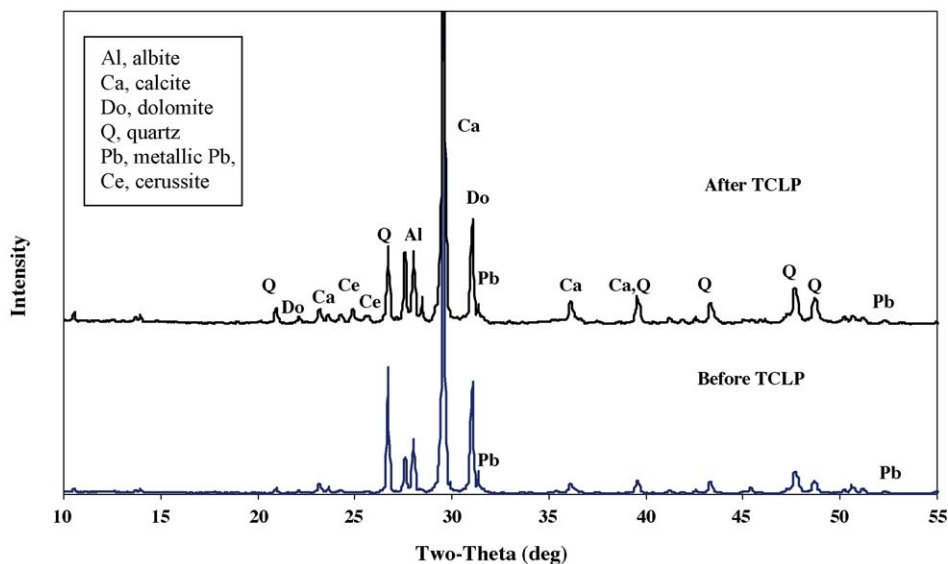| Firing ranges	Actual TCLP Pb (mg/L)	Predicted TCLP Pb (mg/L)	Predicted precipitate	Predicted Pb leachability ratio (%)
FIGS	16.5	3.1	Cerussite	2
PATF	594.0	449.4	Hydrocerussite	33
FDR15	50.2	51.3	None	100
PAMR	10.7	0.31	Cerussite	0.01

Fig. 5. XRPD patterns of PAMR soil samples before and after TCLP, showing persistence of metallic Pb and formation of cerussite induced by TCLP leaching.

lead-to-carbonate in the solid, which is much higher in the PATF soil compared to the FIGS and PAMR soils. The formation of cerussite requires 1:1 stoichiometry of Pb and carbonate, while the stoichiometry of hydrocerussite (3:2) requires less carbonate to bind the same amount of Pb. Moreover, the high total Pb concentration in PATF soil (Table 5) and the TCLP pH also favored hydrocerussite formation. The predicted soluble Pb in this case is 33% of the total Pb, due to the lower pH, as the well as the limited availability of carbonate in the PATF soil as compared to the high Pb content.

The reason for the difference in the Pb concentrations for the FIGS soil could not be clearly established, as no kinetic data were available for this soil. Since the difference between the predicted and the actual TCLP Pb concentration is relatively small, it is considered that a combination of the aforementioned reasons could, again, account for the higher concentration observed in the actual TCLP results. The geochemistry of this soil is complicated, as evidenced by the XRPD data and such differences are within the range of error of a geochemical model. Based on the FIGS soil modeling results, cerussite formed at a pH of 5.8, and controlled Pb leachability even though the sulfate concentration was much higher compared to the carbonate concentration (19,000 mg/kg sulfate versus 4800 mg/kg carbonate). No anglesite [$PbSO_4$] was predicted to form, and all sulfate remained in solution due to the instability of gypsum at pH 5.8. This indicated that the formation of lead carbonate was the thermodynamically favorable reaction even at this relatively low pH. Overall, only 2% of the available Pb was predicted to remain in solution in the TCLP according to the model. It should be also noted that this result was not affected by varying the sulfate concentration from 19,000 mg/kg to 38,000 mg/kg, as previously noted.

The best agreement was obtained for the FDR15 soil which intuitively makes sense, given the fact that it contained 100% quartz (Table 3), the least amount of major elements and the least organic carbon and carbonate contents (Table 4). Cerussite also controlled TCLP Pb leachability in the FDR15 soil; in this case,

however, through its dissolution. The relatively low content of Pb and carbonate (Table 4), coupled with the low post-tumbling TCLP pH (Table 5) readily explains the fact that 100% of the Pb was released during TCLP leaching. The relatively low Pb and carbonate contents rule out kinetic limitations as being relevant, therefore enabling complete dissolution of all Pb within the 18 h of TCLP leaching at pH < 5, where cerussite is highly soluble. Consequently, Pb leachability in this soil was mainly controlled by dissolution reactions at the equilibrium pH condition.

Based on the above discussion, it can be concluded that the model generally reflects the actual mechanisms that are responsible for Pb speciation in the TCLP test. More specifically, the model shows that precipitation/dissolution reactions are principally responsible for TCLP Pb leachability in the firing range soils, and that the carbonate species are predominant and control Pb concentrations in the leachate. Modeling was accurate in predicting Pb TCLP leaching when no kinetic limitations existed during TCLP testing (i.e., equilibrium was achieved within 18 h for the FDR15 soil). More importantly, the model-predicted Pb TCLP leachability can be accurate without considering surface sorption effects. In this study, based on the geotechnical, mineralogical and total analyses data and interpretations, it was initially hypothesized that incorporating sorption effects for the more fine-grained soils (FIGS and PATF) would be necessary in order to obtain accurate model-based predictions of Pb leachability. However, the regime of Pb speciation (i.e., Pb already present as cerussite and in its metallic form which mainly converts to cerussite upon TCLP testing) and the TCLP post-tumbling pH both point to a precipitation–dissolution as the dominant mechanism (instead of sorption) controlling Pb TCLP leachability. Recall that the worst fit between predicted and actual TCLP results were associated with the PAMR soil, not because of its fines content (4.8%), but owing to its mineralogy. While sorption phenomena may play an important role for Pb speciation under field conditions or in other tests with different experimental conditions, it seems that precipitation/dissolution
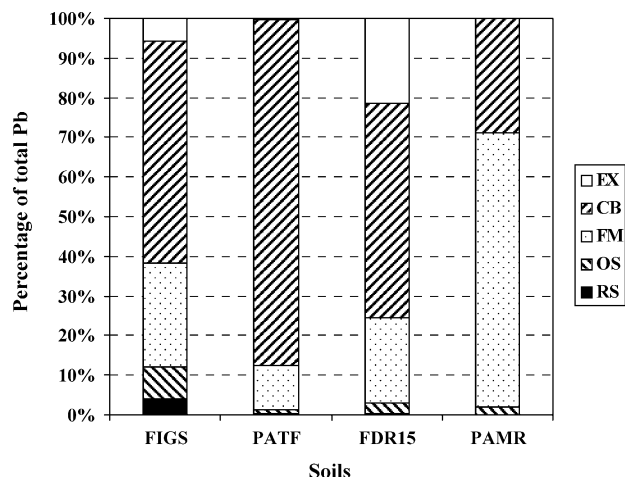
Fig. 6. Sequential extraction results of Pb in firing range soils. EX, exchangeable; CB, carbonate; FM, iron and manganese oxides; OS, organic matter + sulfides; RS, residual.

reactions, and more specifically carbonation, dominate Pb speciation under TCLP conditions. This is due to the acidic conditions imposed by the test, as well as due to the high L:S ratio (20), which favors the dissolution of amorphous material, such as Fe, Al hydroxides that, in turn, favors sorption phenomena, as well as the release of species (namely Pb^{2+} and CO_3^{2-}) into solution and their ultimate precipitation as lead carbonate. The agreement between actual versus predicted Pb leachability ratios for the coarser-grained soils (FDR15 and PAMR) revealed the same mechanisms, and emphasized the importance of mineralogy as key inputs to the model to achieve high accuracy.

More importantly, Tables 5 and 6 show that as the TCLP post-tumbling pH increases, Pb leachability ratio values (actual as well as model-predicted) decrease, pointing to a reduced Pb mobility, thus highlighting the dominating influence of pH in Pb TCLP leaching [24]. TCLP Pb leachability for the firing range soils seems to always be controlled by precipitation/dissolution reactions. Sorption mechanisms could also play a significant role when a significant fines (<75 μm) content is present, but only at elevated pH. Lead carbonates, the predominant Pb weathering by-products, are susceptible to dissolution during TCLP testing if the system pH is less than about 5. Overall, geochemical modeling can reliably predict equilibrium Pb TCLP leaching once the relevant modeling inputs are incorporated (TCLP post-tumbling pH, soil carbonate content, total analyses results, etc.), thus enabling assessments for predicting the relative magnitude of site-specific Pb-related environmental compliance issues in firing range soils. The key drawback is that Visual MINTEQ under-predictions may occur if mineralogical effects are not properly incorporated (i.e., PAMR soil).

3.3.5. Sequential extraction test (SET)

The SET results presented in Fig. 6 suggest that Pb partitioning is not similar among the firing range soils. With the exception of the PAMR soil, carbonates appear to be the most important phase impacting Pb. This is to be expected, as the main metallic Pb transformation product identified in all the soils was lead carbonate, as previously discussed.

Specifically, for the FIGS soil, Pb partitioned in the different fractions as: CB > FM > OS > EX > RS, with more than 95% of the extracted Pb being associated with the CB and FM fractions. The hypothesized role of the relatively high concentrations of Fe and Mn present as amorphous ferromanganese oxides in the FIGS soil (Fig. 1, Table 4) appears to be confirmed by the SET result showing high Pb partitioning (∼25%) in the Fe–Mn oxides phase.

Pb partitioning in the PATF soil was ordered as follows: CB > FM > OM > RS > EX. Similar to FIGS, more than 90% of Pb was concentrated between the CB and FM fractions, and Pb was mainly associated with the carbonates (CB). This finding was also confirmed by XRPD (Table 3) and SEM (Fig. 2c) both pointing to the presence of lead carbonate (cerussite). Also, carbonate content analyses (Table 4) suggested that the measured carbonate was, to some degree, associated with cerussite. As 2.7% Pb was measured by total analyses in the soil (Table 4), it seems that about 11% of the Pb was present in its carbonate form (Table 3). These results contradict the SET results, which quantified the Pb association with the CB fraction to a level higher than 80%. The FM fraction follows CB in concentrating about 15% of the total amount of Pb. As previously illustrated by XRPD and total analyses, possibly goethite (FeOOH) and certainly aluminum hydroxides (i.e., boehmite and bayerite) may also comprise available surfaces for Pb sorption in the PATF soil. It may be that part of the sorbed Pb, presumably on the alumina surfaces, and probably some metallic Pb was erroneously assigned to the carbonate fraction by the Tessier method [27–29].

The FDR15 soil had the highest exchangeable (EX) fraction (21%) among the firing range soils tested. Much of this is likely the result of desorption of Pb from quartz surfaces which are highly exchangeable. Moreover, the pH of the FDR15 was found to be acidic, indicating that Pb sorption would be weak and Pb would be prone to leaching during the first step of extraction. The majority of Pb in the FDR15 soil (54%) was assigned to the carbonate phase of the soils by SET which seems disproportionate based on the FDR15 soils' extremely low carbonate content (Table 4). This suggests that any metallic Pb in the soil must have weathered during the test itself and formed Pb carbonate by-products. This type of process was evidenced by XRPD analyses of weathered bullet crust particles that showed both metallic Pb and cerussite (Fig. 3). It should be stressed that the pH regime at these surfaces is locally different than the overall acidic environment, as the presence of Pb and the formation of Pb oxides releases alkalinity, raising the pH locally enough for cerussite to form on the weathered surface. The total carbonate content was measured at 0.01% (Table 4), which could bind 0.03% Pb as lead carbonate, or about 30% of the total Pb (Table 4). This enhances the assumption that carbon influx (i.e., from leaching solutions) during the test was necessary in order to account for 54% of the Pb in the carbonate fraction. It should be stressed, however, that the low total concentration of both species, Pb and carbonate, introduces higher uncertainties in the mass balances as compared to the previous cases. Almost 75% of Pb from the FDR15 soil was removed by the first two SET extraction steps. During the third extraction step Pb was released even further. Overall, during the first three SET steps about 98% of the total Pb present

was released (Fig. 6). This finding is in good agreement with the very high TCLP Pb to total Pb leachability ratio results (97.9% for actual and 100% for model-predicted) for the FDR15 soil, as shown in Tables 5 and 6. However, since the FDR15 soil did not contain substantial quantities of ferromanganese oxides (Table 4), the key phases supposedly attacked during the third SET step, it appears that SET is unable to provide a precise evaluation of soil–metal interactions and Pb speciation.

The PAMR soil had the lowest TCLP Pb concentrations and Pb leachability ratio (Tables 5 and 6). Pb leaching by SET had the following order: FM > CB > OS ≥ RS ≥ EX. Only 25% of the Pb was associated with the carbonates, whereas about 70% of Pb was bound to Fe–Mn oxides. However, the actual Fe and Mn contents were quite low based on the total chemical analyses results (Table 4) and the XRPD analysis showed no amorphous Fe–Mn humps (Fig. 5). Therefore, Fe–Mn oxide mineral phases were most likely not responsible for the Pb leaching behavior during the third SET extraction step. Conversely, metallic Pb was the only Pb mineral identified in the initial sample by XRPD (Table 3, Fig. 5). Following the TCLP test, newly formed cerussite was observed based on the XRPD pattern of the TCLP residue from the PAMR soil (Fig. 5). It should also be noted that metallic Pb was still identified within the TCLP soil residuals (Fig. 5). Jointly, these findings must be used to reconcile actual Pb speciation and leaching behavior in the PAMR soil. More specifically, 2.2% of the 4.9% total Pb (Table 4) in the PAMR soil was present in its metallic form, as estimated by Rietveld analysis (Table 3). The Tessier method does not account for the presence of metallic Pb, unless it is leached exclusively in the residual fraction. This is, however, rather unlikely, as upon the incremental acid addition during the SET last four steps, pH would incrementally decrease, thus solubilizing Pb as free Pb^{2+} cation. In this case, soil buffering capacity controls which SET step drops the pH sufficiently for metallic Pb to solubilize. In other words, it is difficult, if not impossible, to associate actual metallic Pb with any of the operationally defined SET fractions. Hence, the Tessier method cannot reliably determine Pb speciation in firing range soils because it will likely attribute metallic Pb to other phases. The following paragraphs provide more detail on this phenomenon which appears to be an artifact of the SET method when applied to firing range soils.

The first SET step employing $MgCl_2$ was not likely to significantly impact the mostly metallic Pb (Table 3) in the relatively high pH (pH 8.7; Table 2) PAMR soil. During the second SET step, when weak acid was applied to the soil, Pb was partially released from its metallic phase. Concomitant dissolution of calcite and dolomite in the soil, provided sufficient carbonate to react with aqueous Pb^{2+} to form cerussite. Moreover, the high buffering capacity of this soil system inhibited a pH decrease below 6. Consequently, Pb leaching appeared to be significantly limited, most likely due to the low solubility of the newly formed cerussite at pH levels above 6. Similarly, Dermatas and Meng [30] showed that at pH < 9 Pb release was mainly controlled by the solubility of the Pb transformation products. Also, calcite and dolomite surfaces could provide enough surface sites for Pb adsorption, specifically by an inner-sphere mechanism [31].

Consequently, during the second SET extraction, Pb release was probably inhibited by the formation of cerussite. More pointedly, Pb was not removed from its carbonate phase; instead it formed more $PbCO_3$ with the dissolved CO_3^{2-}. During the third SET step, the system pH decreased significantly, probably overcoming the soil buffering capacity. Moreover, the L:S ratio was increased in the third SET step to 20:1 from 8:1 for the first two SET steps, and the temperature was increased 70 °C, thus significantly facilitating Pb and carbonate extraction during the third SET step. Owing to the considerable shifts in contact time, L:S ratio and pH occurring during the third SET extraction step, Pb was leached from the newly formed cerussite and calcite- and/or dolomite sorption sites. As such, the SET procedure misattributes the leached Pb to an FM phase. Overall, the significant presence of calcite and dolomite was believed to be the predominant factor influencing Pb speciation in the PAMR soil, in that it provided a high buffering capacity for the entire soil system, a sufficient carbonate source to form cerussite, and to a lesser extent, enough surfaces for Pb adsorption.

Collectively, the data and trends produced by various investigative techniques for soil and the mineralogical analyses suggest that that soil parameters and geochemistry greatly affect Pb speciation and leachability in firing range soils. More specifically, the SET, as proposed by Tessier et al. [21], even though it can provide some useful information on Pb speciation and release, it cannot reliably distinguish the underlying mechanisms without supplemental mineralogical and chemical analyses. Moreover, SET alone cannot adequately explain or help predict the levels of regulatory (TCLP), and possibly otherwise, Pb release. Alternatively, based on preliminary soil mineralogical evaluations and geochemical analyses a more targeted, soil-specific SET approach can be applied. It is also important to note that Cao et al. [9] demonstrated that Pb leachability was highest in firing range soils where Pb was primarily associated with the carbonates and lowest when Pb was associated with the residual fraction, a finding that was not confirmed during the present study. A significant Pb association with the residual fraction of the firing range soils tested was not observed and the lowest Pb leachability was measured for the soil (PAMR) with the lowest amount of Pb associated with the residual fraction. Conversely, Pb was primarily associated with the carbonate fraction regardless of Pb leachability levels, again, with the exception of the PAMR soil. For the PAMR soil, even though a significant amount of metallic Pb (2.2%) was present, and despite the low levels of Fe and Mn (Table 4), the SET assigned Pb to the FM fraction and not to the RS fraction. For the FIGS and PATF soils, which contained significant Fe–Mn fractions (Table 4), the Pb associated with the FM phase as estimated by SET was not commensurate. In fact, the FDR15 soil had the lowest Fe–Mn content (Table 4), but showed comparable levels of extractable Pb associated with the FM fraction as the FIGS and PATF soils. Moreover, as relevant research has demonstrated, the SET overestimates the labile phases of soil Pb, particularly the quantity of Pb associated with the carbonate fraction which is further linked to the Pb fragment size. Hence, the utility of the Tessier SET procedure remains doubtful for the analysis of firing range soils.

4. Summary and conclusions

Overall, the geotechnical, mineralogical and chemical analyses (multiple lines of evidence) were all in very good agreement and pointed to two possible Pb retention mechanisms: carbonation (for all soils) and sorption (for the FIGS, PATF and PAMR soils). The modeling results showed that Pb TCLP release was controlled by dissolution/precipitation reactions in all four soils and, more specifically, by the amount of precipitated lead carbonate (cerussite and hydrocerussite). Furthermore, the TCLP pH was a significant factor in Pb leachability, as it controls the equilibrium concentrations of precipitated lead carbonate and, consequently, Pb in solution. Overall, the geochemical model pointed to an apparent absence of sorptive phenomena in the TCLP test, regardless of the nature of the soil, i.e., the fines content, the presence of clays, ferromanganese oxides and aluminum hydroxides. While sorption phenomena may play an important role for Pb speciation under field conditions or in other tests with different experimental conditions, it seems that precipitation/dissolution reactions and more specifically carbonation, dominate Pb speciation in the TCLP. These observations led to the conclusion that, once the total metal and carbonate concentrations have been measured and the TCLP pH is known, geochemical modeling can be employed as an assessment tool to evaluate the Pb TCLP equilibrium concentration.

A reliable determination of Pb speciation by the Tessier method was not possible for firing range soils due to the significant role of soil chemistry, mineralogy and buffering capacity, and their control of the prevailing Pb speciation in both the TCLP and SET tests. The presence of high amounts of metallic Pb in firing range soils renders the Tessier method inadequate, as metallic Pb transformations are obscured by one or more SET steps, depending on the aforementioned soil characteristics. Thus, SET lumps the extractable Pb into predetermined phase categories which may not be truly representative of the actual soil mineralogy or dominant forms of Pb in the soil. This has serious implications for the validity of the Tessier SET technique for application to firing range soils. A thorough geotechnical, mineralogical and chemical investigation of firing range soils, supplemented by geochemical modeling, emerged as a more accurate and comprehensive approach to assess Pb speciation and mobility in firing range soils.

More succinctly, the lessons learned with respect to reliably assessing Pb release in firing range soils can be summarized as follows:

- Sieve analysis results, specifically the presence of a high fines content, may point to the availability of soil sorption sites for Pb immobilization. However, the determination of soil mineralogy is essential to verify and quantify the presence of active clays and amorphous and/or poorly crystallized metal oxides and hydroxides that will contribute to Pb immobilization. Feldspars and other non-clay and non-reactive fines will not significantly affect Pb leaching.
- Bulk mineralogy as determined by XRPD may reveal Pb species only if Pb concentrations are high enough (i.e., above the XRPD detection limit for the specific Pb species). XRPD of discrete soil features, guided by optical microscopy observations and complemented by SEM observations, are critical in further identifying aspects of Pb speciation that cannot be readily discerned by bulk XRPD.
- When TCLP (or other leaching tests) are used, employing the Pb leachability ratio (TCLP Pb/total Pb) provides an effective assessment of Pb leaching potential. Geochemical modeling can be reliably used to predict TCLP Pb release from firing range soils as long as equilibrium is attainable and mineralogy is properly incorporated. The main reason for this is that it appears that during the TCLP lead carbonate precipitation/dissolution reactions dominate the system over sorption reactions occurring at crystalline and/or amorphous solid interfaces. Thus, modeling can be used as a rapid assessment tool to evaluate the magnitude of site-specific Pb-related environmental problems in firing range soils.
- The SET appears unable to thoroughly identify Pb speciation and leaching behavior in firing range soils. The method fails to reliably address critical Pb species, such as metallic Pb and Pb sorbed onto other surfaces other than ferromanganese oxides and organic matter (i.e., active clays and aluminum hydroxides).

References

[1] D.R. Lillquist, F. Sullivan, J.W. Bowles, D. Meservy, T. Aldrich, Y.C. Lewis, A comparison of environmental sample methods for estimating soil lead at trap shooting ranges: the effects of pellet and nonpellet lead, Appl. Occup. Environ. Hyg. 13 (12) (1998) 824–828.
[2] D. Dermatas, N. Menounou, M. Dadachov, P. Dutko, G. Shen, X. Xu, V. Tsaneva, Lead leachability in firing range soils, J. Environ. Eng. Sci., in press.
[3] A. Tessier, P.G.C. Campbell, M. Bisson, Particulate trace metal speciation in stream sediments and relationship with grain size: implication for geochemical exploration, J. Geochem. Explor. 6 (1982) 77–104.
[4] R.N. Yong, B.P. Warkentin, Y. Phadungchewit, R. Galvez, Buffer capacity and lead retention in some clay materials, Water Air Soil Pollut. 53 (1990) 53–67.
[5] R.N. Yong, Y. Phadungchewit, pH Influence on selectivity and retention of heavy metals in some clay soil, Can. Geotech. J. 30 (1993) 821–833.
[6] R. Bruell, N.P. Nikolaidis, R.P. Long, Evaluation of remedial alternatives of lead from shooting range soil, Environ. Eng. Sci. 16 (5) (1999) 403–414.

[7] Z. Lin, B. Comet, U. Qvarfort, R. Herbert, The chemical and mineralogical behavior of Pb on shooting range soils from Central Sweden, Environ. Pollut. 89 (3) (1995) 303–309.

[8] S. Jorgensen, M. Willems, The transformation of lead pellets in shooting range soils, Ambio 16 (1987) 11–15.

[9] X. Cao, L.Q. Ma, M. Chen, D.W. Hardison, W.G. Harris, Lead transformation and distribution in the soils of shooting ranges in Florida, USA, Sci. Total Environ. 307 (2003) 179–189.

[10] X. Cao, L.Q. Ma, M. Chen, D.W. Hardison, W.G. Harris, Weathering of lead bullets and their environmental effects at outdoor shooting ranges, J. Environ. Qual. 32 (2003) 526–534.

[11] D. Dermatas, M. Dadachov, P. Dutko, N. Menounou, P. Arienti, G. Shen, Weathering of lead in Fort Irwin firing range soils, Global Nest (Environ. Sci. Technol.): Int. J. 6 (2) (2005) 73–84.

[12] A. Scheinost, Lead corrosion in soils: a literature review, in: World Symposium on Lead in Ammunition, The World Forum on the Future of Sport Shooting Activities (WFSA) Symposium Proceeding, 2004, pp. 135–145.

[13] ASTM, Annual Book of ASTM Standards, vol. 4.08, American Society for Testing and Materials. Soil and Rock, 2000.

[14] Material's Data Inc., Jade 2004, Version 7.1, California, USA.

[15] Powder Diffraction File, PDF-2 Database Release 1998, Announcement of new database release, International Centre for Diffraction Data (ICDD).

[16] Inorganic Crystal Structure Database, Fachinformationszentrum Karlsruhe, Germany, 2004.

[17] H.M. Rietveld, A profile refinement method for nuclear and magnetic structures, J. Appl. Crystal. 2 (1969) 65–71.

[18] A. Walkley, I.A. Black, An examination of the Degtjareff method for determining organic carbon in soil: effect of variations in digestion conditions and of inorganic soil constituents, Soil Sci. 63 (1934) 251–263.

[19] U.S. EPA, SW-846, Method 3050B, Acid Digestion of Sediments, Sludges, and Soils.

[20] U.S. EPA, SW-846, Method 1311, Toxicity Characteristic Leaching Procedure.

[21] A. Tessier, P.G.C. Campbell, M. Bisson, Sequential extraction procedure for the speciation of particulate trace metals, Anal. Chem. 51 (7) (1979) 844–851.

[22] J.P. Gustafsson, Visual MINTEQ ver. 2.30, KTH, Royal Institute of Technology, Sweden, 2004.

[23] C.E. Halim, J.A. Scott, R. Amal, S.A. Short, D. Beydoun, G. Low, J. Cattle, Evaluating the applicability of regulatory leaching tests for assessing the hazards of Pb-contaminated soil, J. Hazard. Mater. B120 (2005) 101–111.

[24] D.S. Kosson, H.A. van der Sloot, F. Sanchez, A.C. Garrabrants, An integrated framework for evaluating leaching in waste management and utilization of secondary materials, Environ. Eng. Sci. 19 (2002) 159–204.

[25] C.E. Halim, J.A. Scott, H. Natawardaya, R. Amal, D. Beydoun, G. Low, Comparison between acetic acid and landfill leachates for the leaching of Pb(II), Cd(II), As(V), and Cr(VI) from cementitious wastes, Environ. Sci. Technol. 38 (2004) 3977–3983.

[26] A. Ghosh, M. Mukiibi, W. Ela, TCLP underestimates leaching of arsenic from solid residuals under landfill conditions, Environ. Sci. Technol. 38 (2004) 4677–4682.

[27] M. Raksasataya, A.G. Langdon, N.D. Kim, Assessment of the extent of lead redistribution during sequential extraction by two different methods, Anal. Chim. Acta 332 (1996) 1–14.

[28] J.L. Gómez Ariza, I. Giráldez, D. Sánchez-Rodas, E. Morales, Selectivity assessment of a sequential extraction procedure for metal mobility characterization using model phases, Talanta 52 (2000) 545–554.

[29] V. Ettler, A. Vanek, M. Mihaljevic, P. Bezdicka, Contrasting lead speciation in forest and tilled soils heavily polluted by lead metallurgy, Chemosphere 58 (10) (2005) 1449–1459.

[30] D. Dermatas, X. Meng, Utilization of fly ash for stabilization/solidification of heavy metal contaminated soils, J. Eng. Geo. 70 (3–4) (2003) 377–394.

[31] A. Rouff, X-ray absorption spectroscopic evidence for the formation of Pb(II) inner-sphere adsorption complexes and precipitates at the calcite–water interface, Environ. Sci. Technol. 38 (2004) 1700–1707.